



Geochemical and Isotopic Constraints on the Recharge and Salinization Origin of Groundwater Aquifers in El Rina–Nihayaat, South Sinai, Egypt

Mustafa Eissa ^{a*}

^a *Desert Research Center, Division of Water Resources and Arid Land, Hydrogeochemistry
Department, Cairo, Egypt.*

Author's contribution

The sole author designed, analyzed, interpreted and prepared the manuscript.

Article Information

DOI: 10.9734/AJEE/2024/v23i3529

Open Peer Review History:

This journal follows the Advanced Open Peer Review policy. Identity of the Reviewers, Editor(s) and additional Reviewers, peer review comments, different versions of the manuscript, comments of the editors, etc are available here: <https://www.sdiarticle5.com/review-history/112097>

Original Research Article

Received: 18/08/2023

Accepted: 24/01/2024

Published: 27/01/2024

ABSTRACT

The Sinai Peninsula is located in the arid regions of Egypt where groundwater is the sole source for drinking and irrigation and future development. Regular assessment of the geochemical processes governing the groundwater quality is important in arid regions and paleo-aquifers. This research focuses on investigating the groundwater sustainability of the Upper Cretaceous Aquifer (UCA) located at El Rina–Nihayaat area, Southwestern Sinai Peninsula. The study aims to evaluate the main source of groundwater recharge and investigate factors deteriorating groundwater quality. The study is based on the geochemical and isotopic analyses of 31 groundwater samples tapping the UCA. The groundwater flows toward the Gulf of Suez. The groundwater salinity ranges from 1078 mg/L to 13090 mg/L indicating brackish to saline water. Two main water types have been delineated: Cl-Na and Cl-Ca indicating the final stage of groundwater evolution and leaching and dissolution of aquifer matrix of marine origin. The spatial distribution of the groundwater salinity and major ions (Na^+ , K^+ , Ca^{2+} , Mg^{2+} , SO_4^{2-} , and Cl^-) increase toward the Gulf which coincides with the

*Corresponding author: E-mail: mustafa.eissa@drc.gov.eg;

direction of the groundwater flow, while bicarbonate increases toward the upstream watershed. Most of the groundwater samples tapping the UCA are depleted with the isotopic content of the stable isotopes where they range from -4.43 ‰ to -6.37 ‰ for $\delta^{18}\text{O}$ and -28.3 ‰ to -40.2 ‰ for $\delta^2\text{H}$. The groundwater samples are depleted relative to the recent rainwater and enriched to the Nubian Sandstone located underneath the UCA indicating mixing from both source(s). The mixing estimated percentages from the recent rainwater using calibrated geochemical NETPATH model range between 48.6% to 88.5% while the upward Leakes from the Nubian water ranges between the recent rain and the paleo-Nubian water ranges between 48.6 % and 88.5 % from the meteoric rainwater, while the upwelling recharge from the paleo-Nubian groundwater ranges between 11.5 % to 51.4 %. The factorial analyses indicate three main factors governing the geochemistry of groundwater in the UCA: including water-rock interactions, meteoric recharge from annual precipitation, and upward leakages from the underneath paleowater. Further exploration for the UCA is recommended to determine the promising zones receiving a considerable amount of the recent rainfall.

Keywords: El Rina–Nihayaat; South Sinai; groundwater chemistry; stable isotopes; geochemical modelling; statistical factorial analyses.

1. INTRODUCTION

The El Rina–Nihayaat Watersheds are in the South Sinai Peninsula, draining toward the Gulf of Suez. The total area of the two basins is about 170 Km². The study area is located within the arid zone, where the inhabitants suffer from scarcity of water resources for human drinking and agriculture. The development in arid regions depends mainly on groundwater availability. Sinai Peninsula comprises three main aquifers: Quaternary aquifer, Upper Cretaceous aquifer (UCA), and Lower Cretaceous aquifer (LCA) [1]. Consequently, proper assessment of the (UCA) is essential to ensure sustainable development. The Upper and Lower Cretaceous are transboundary aquifers extended outside the western political boundary of Egypt to Palestine [2,3]. Many studies were conducted for the UCA [4-7]. However, the UCA is ill-constrained where few studies were conducted due to the geologic complexity [8,9]. Ibrahim et al. [10] reported that to avoid aquifer depletion of the Nubian aquifer in Sinai, the convenience of the UCA as an alternative source of freshwater should be explored. Additionally, the relation between the Upper and the Lower Cretaceous must be defined. Many authors considered they are isolated due to discrepancies in groundwater level and the intercalations of confining impermeable shale and clay layers [4,5] however other research confirmed that they are hydraulically connected through the deep-seated fault zones [11].

Hydrogeology and hydrogeochemistry are important for understanding groundwater flow hydrodynamics and evaluating groundwater

potential assessment and management [12-14]. Recently, more than forty groundwater wells tapping the UCA have been drilled at the upstream watershed during 2019 initiating the expansion of agricultural development. Therefore, the hydrological parameters and subsurface geological data are important to assess the water level, quality, and quantity, of groundwater in the study area. The wells' data could be useful for determining the potential zones of the aquifer used for sustainable development. In arid regions, groundwater geochemistry and isotopes are fundamental components of hydrogeology, providing critical insights into the origin, movement, and quality of subsurface water resources [15,16]. This research investigates the chemical composition of groundwater and the use of isotopic tracers to unravel the hydrological cycle and understand water-rock interactions. Understanding the composition helps assess water quality, identify sources of contamination, and study natural processes influencing water chemistry [17]. Isotopic analysis involves studying the abundance of stable (e.g., oxygen-18, deuterium) in water molecules. Isotopic tracers help determine the origin, age, and flow paths of groundwater [18,19]. They can differentiate between different sources of water (meteoric, recycled, or ancient) and provide insights into recharge mechanisms and flow dynamics [20,21].

This study has been conducted to investigate the subsurface aquifer and identify the groundwater flow system, geochemistry as well as to determine the main source of groundwater recharge and salinization and accordingly,

suitable areas for different purposes could be determined. The UCA is underheated by the Nubian Sandstone aquifer and cropping out at the central and North Siani Peninsula. Therefore, hydrogeochemical data in conjunction with isotopes have been utilized to investigate the recharge source and determine factors affecting the groundwater quality.

1.1 Study Area

The study area is in the southeastern part of the Sinai Peninsula; it extends between longitudes 32.4 and 33.0 E and latitudes 29.6 and 30.0 N.

It covers an area of 55 km² (Fig. 1). The area is considered a part of an arid climate which is mainly dominated by hot summers and cold winters and scarce rainfall (30 mm/year) [22]. The ground elevation is 229 m above sea level toward the east, close to the main water divide of Wadi El Arish, to zero level at the Gulf of Suez coastal line to the East. The ground surface slopes toward the Western side with a mid-slope of 1 m/km. The area comprises several geomorphic units, including table land area represented by the El-Tih Plateau which is dissected by drainage basins and a coastal plain downstream.

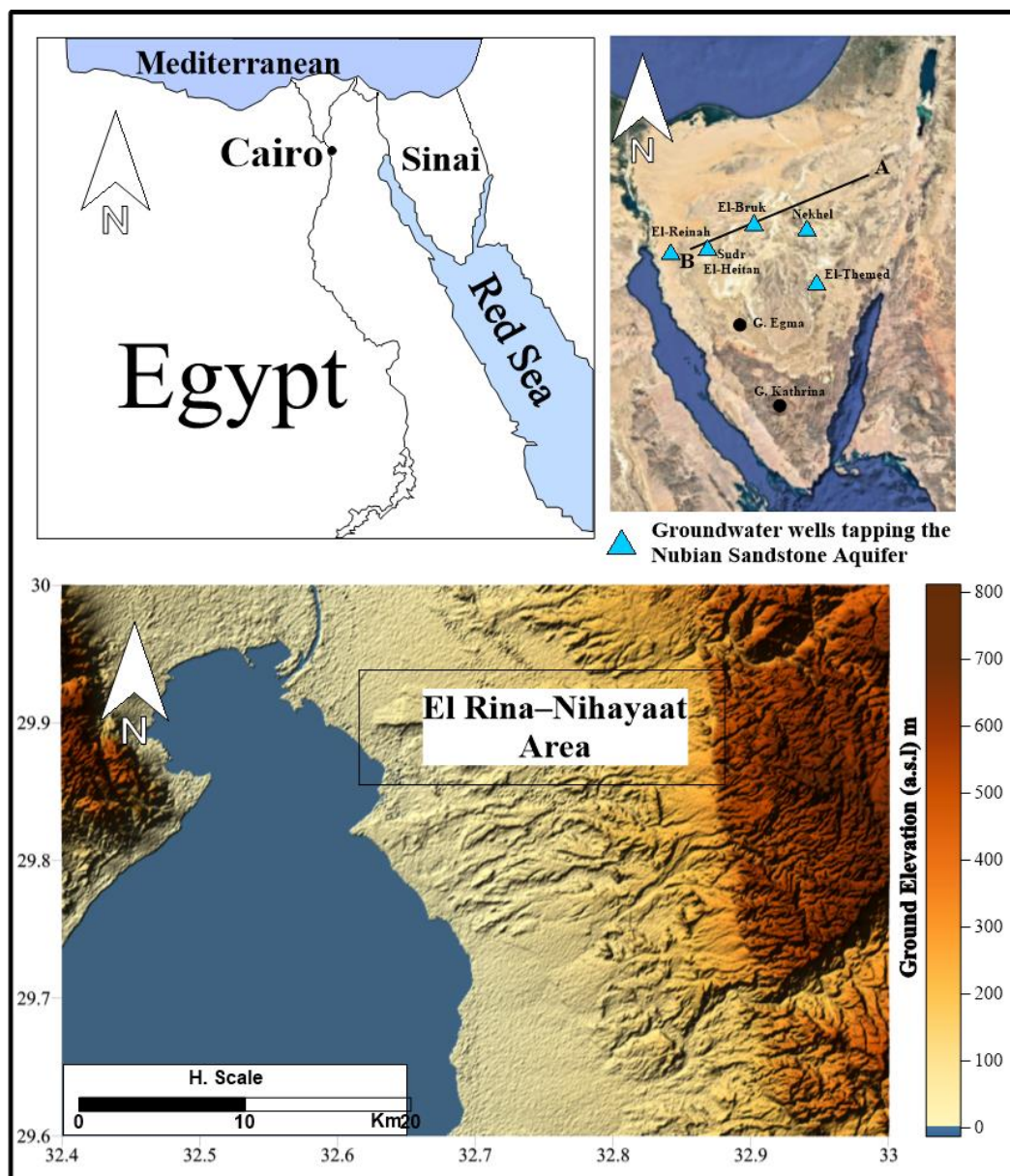


Fig. 1. Location maps of the study area

2. METHODOLOGY

A field trip was carried out in February 2022, during the trip 31 groundwater samples were collected from the study area. The physical groundwater properties were measured during the field trip, including pH, Ec ($\mu\text{mohs}/\text{cm}$), and T ($^{\circ}\text{C}$). In the field site, each well was purged before sampling and then the pH was measured using Apera Instruments PH400 with an accuracy of ± 0.01 for pH and $\pm 0.5^{\circ}\text{C}$ for temperature. The conductivity has been measured using a multi-range EC meter with a HI76302W probe, with a range of 0.0 to 199.9 mS/cm. Instruments were calibrated twice daily during the field trip. The major ions were carried out at the Desert Research Center, Water Center Laboratory in Cairo, Egypt using the analytical methods described by Geo Engineers [23], Fishman and Friedman [24]. The depth to water from the ground surface has been measured using Solinst model 107 TLC level meter sounder. Analytical major cations (Ca^{2+} , Mg^{2+} , Na^{+} , K^{+}) and major anions (SO_4^{2-} , Cl^{-}) were measured at the Desert Research Central Laboratory using Thermo Scientific Dionex ICS-1100 Ion Chromatography System (Table 1). The groundwater alkalinity has been determined using titration against the dilute solution of H_2SO_4 using Phenol Phthalein and Methyl orange as indicators [25]. For quality assurance, the electrical charge balance for the major cations and major anions has not exceeded $\pm 5\%$. The stable isotopes, including

$\delta^{18}\text{O}$ and $\delta^2\text{H}$, were determined in the UC Davis laboratory in California using the IAEA Standards (V-SMOW) methods [26,27]. The saturation indices (SI) for groundwater are calculated using the NETPATH software [28,29]. The statistical analysis has been used to determine the dominant geochemical processes therefore, the Keyplot software [30] has been used to extract the factorial using the geochemical analyses as data input.

2.1 Geology and Hydrogeology

The area comprises rocks ranging in age from the Paleozoic to Quaternary deposits [31-36] (Fig. 2). The surface is covered by the alluvial deposits which formed mainly of silt, sand, and gravel that derived from the weathering of the upstream watershed which formed mainly of sedimentary rocks of El-Tih Plateau. The Miocene rocks crop out at the western part of the study area close to the Gulf of Suez and are represented mainly by Ras Malaab which is formed mainly of evaporites intercalated with shale and Gharandal group which comprises clastic marl and reefal carbonates [37]. The Eocene age is represented by the Egma Formation, a moderately bedded marine chalky limestone with chert, and Esna shale Formation which is formed of greenish-gray open marine shale. The Upper Cretaceous is formed mainly of four formations; Galalah, Wata, Matullah, and Sudr formations [4,5,32,38-41].

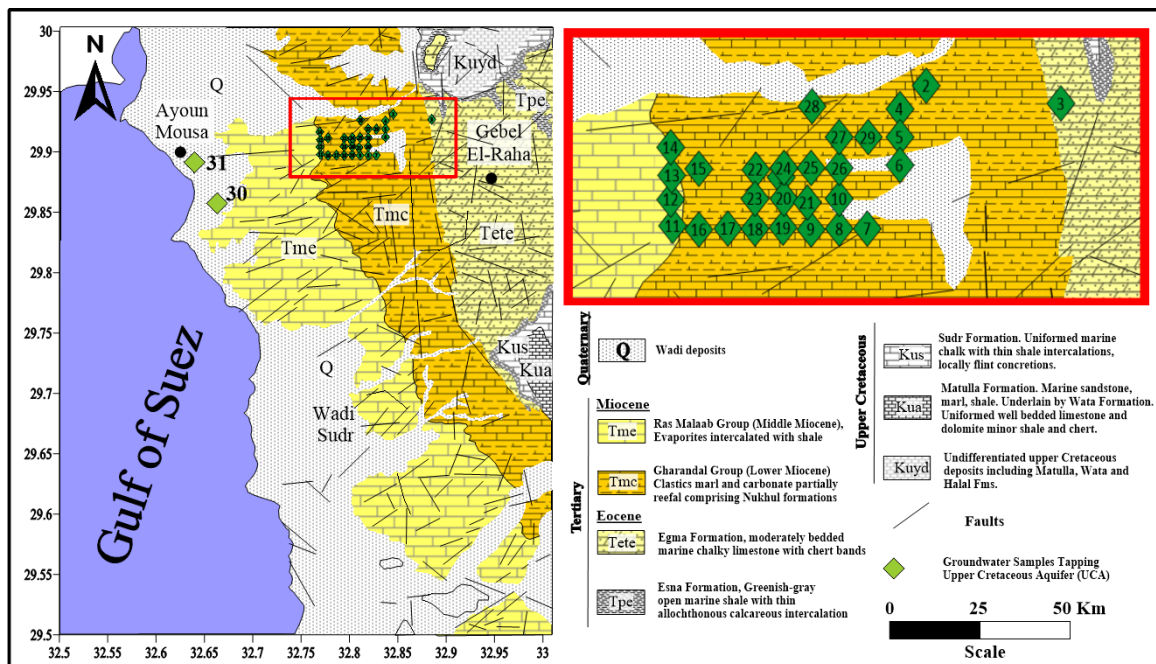


Fig. 2. Geological map of the study area [37]

Table 1. Chemical and isotopic data for groundwater samples in El Rina – Nihayaat area, South Sinai, Egypt (Samples have been collected in February 2022)

No	pH	TDS	Ca	Mg	Na	K	CO ₃	HCO ₃	SO ₄	Cl	δ ¹⁸ O	δ ² H
1	7.29	1186	146.4	118.1	93	34	--	97.4	65.9	679.8	-5.94	-35.2
2	7.44	1114	48.0	72.9	225	33	--	62.6	89.8	614.0	-5.32	-31.1
3	7.79	1120	48.0	55.4	270	30	--	62.6	49.7	636.0	-6.37	-39.1
4	7.25	1592	60.0	62.7	346	63	--	52.2	398.1	636.0	-6.02	-36.2
5	8.19	1123	36.0	80.2	230	19	--	59.1	92.9	636.0	-6.10	-36.5
6	8.06	1144	43.2	64.2	248	31	--	55.6	116.1	614.0	-5.87	-35.2
7	7.85	1161	43.2	75.8	246	35	--	41.7	82.7	657.9	-5.90	-35.3
8	8.32	1078	24.0	72.9	256	34	--	93.9	31.0	614.0	-5.93	-36.3
9	7.81	1404	60.0	102.1	279	47	--	45.2	104.0	789.5	-5.95	-35.6
10	7.55	1126	31.2	75.8	252	32	--	66.1	43.6	657.9	-5.94	-35.4
11	9.02	1275	24.0	51.0	367	36	20.52	27.8	16.4	745.6	-6.03	-35.4
12	8.69	1246	28.8	67.1	305	34	--	52.2	18.1	767.6	-5.87	-35.5
13	8.08	1269	24.0	51.0	348	29	--	59.1	41.6	745.6	-6.02	-36.3
14	4.26	13092	2520.0	1530.9	175	29	--	45.2	42.1	8772.0	-6.06	-35.8
15	7.33	1427	12.0	65.6	398	31	--	69.5	30.4	855.3	-6.08	-36.2
16	7.09	1171	19.2	46.7	326	30	--	34.8	8.7	723.7	-6.18	-36.8
17	8.39	1211	19.2	61.2	324	29	--	66.1	21.3	723.7	-6.04	-35.8
18	8.38	1550	19.2	78.7	348	92	--	80.0	269.8	701.8	-6.07	-35.7
19	8	1307	19.2	72.9	290	87	--	55.6	108.5	701.8	-4.43	-28.3
20	8.42	1179	19.2	75.8	295	25	--	52.2	58.8	679.8	-5.800	-40.2
21	8.32	1343	2.4	93.3	253	120	--	45.2	171.4	679.8	-5.94	-35.2
22	8.43	1280	24.0	58.3	391	30	--	104.3	23.3	701.8	-5.32	-31.1
23	8.44	1272	12.0	65.6	382	31	--	48.7	33.1	723.7	-6.37	-39.1
24	8.46	1205	14.4	36.5	381	26	--	55.6	17.8	701.8	-6.02	-36.2
25	8.78	1332	28.8	11.7	402	92	--	48.7	49.7	723.7	-6.10	-36.5
26	8.59	1382	43.2	53.9	363	66	--	62.6	145.0	679.8	-5.87	-35.2
27	8.27	1135	43.2	17.5	350	31	--	69.5	22.1	636.0	-5.90	-35.3
28	8.2	1141	36.0	83.1	239	27	--	52.2	71.5	657.9	-5.93	-36.3
29	8.11	1222	48.0	51.0	344	36	--	52.2	80.6	636.0	-5.95	-35.6
30	7.69	1566	213.6	81.6	260	36	--	146.0	89.8	811.4	-5.94	-35.4
31	7.14	7354	1440.0	291.6	985	35	--	233.0	56.4	4429.9	-6.03	-35.4
Nekhl-1		2156	116	92	222	21	--	220	485	355	-8.5	-58
Nekhl-5		1150	225	112	200	18	--	221	285	410	-8.76	-57.9
Jica-6		1536	140.3	121.6	252	12.5	--	182.9	559.7	508	-5.9	-42.8

No	pH	TDS	Ca	Mg	Na	K	CO ₃	HCO ₃	SO ₄	Cl	δ ¹⁸ O	δ ² H
							ppm			‰		
Sudr El-Heitan		1472	120	194.6	210	20.7	--	187.9	340.8	374	-8.44	-55.2
El-Bruk-I		2496	64.1	58.3	817	2	--	399.3	54.7	1,240	-9.53	-72.3
Avg Nubian		1762	133	116	340	15	--	242	345	577	-8	-57
Rainwater	7.0	29.15	7.1	0.6	2.3	--	--	14.5	6.4	5.5	-4.37	-21.40
water												

Note: -- means not detected. ppm; part per million (mg/L); and ‰; permille

The Galalah Formation conformably overlies the sandstone facies of the Malha Formation (Lower Cretaceous), it formed mainly of limestone, marl, shale, and sandstone beds of the Cenomanian age. The Wata formation is formed of dolomitic limestone of the Turonian age, the Matallah formation is of limestone, shale, and marl of the Senonian age while the Sudr formation is a marine chalky limestone of Maastrichtian [42].

The UCA aquifer is formed mainly of clastic rocks mainly of fractured limestone and dolomite intercalated with shale interbeds [5,43,44]. The UCA is overlain by the Tertiary (Paleocene, Eocene, Oligocene, Miocene, and Pliocene) and Quaternary formations. The thickness of the aquifer ranges from 300 to 900 meters and the aquifer storativity ranges from 5×10^{-5} to 5×10^{-3} in the confined zones [3,10]. The average hydraulic conductivity is 18.4 m/day, and the transmissivity is 663.7 m²/day [8]. In central

Sinai, the average production from the groundwater wells tapping the UCA ranges from 50 to 70 m³/h, while in the south it decreases to 5 m³/h [4]. The groundwater flow dynamic should be well investigated to study the processes affecting groundwater quality. The ground surface elevation has been estimated using the Digital Elevation Model (STRM-30), and it ranges between 9 m (No. 13) and 205 m (No. 3) above sea level. In the study area, the depth of groundwater was measured during the field trip conducted in February 2022, it ranges between 0.5 m (No. 13) to 68 m (No. 6). The groundwater level has been estimated for all groundwater wells, ranges between 9 m (No. 30) and 196 m (No. 2), and two springs have been detected in the west close to the coastal shoreline. In Fig. 3, the contour map of the groundwater level data shows the groundwater flows from the upstream watershed of Wadi El Rina toward the Gulf of Suez with a slope value of 0.006.

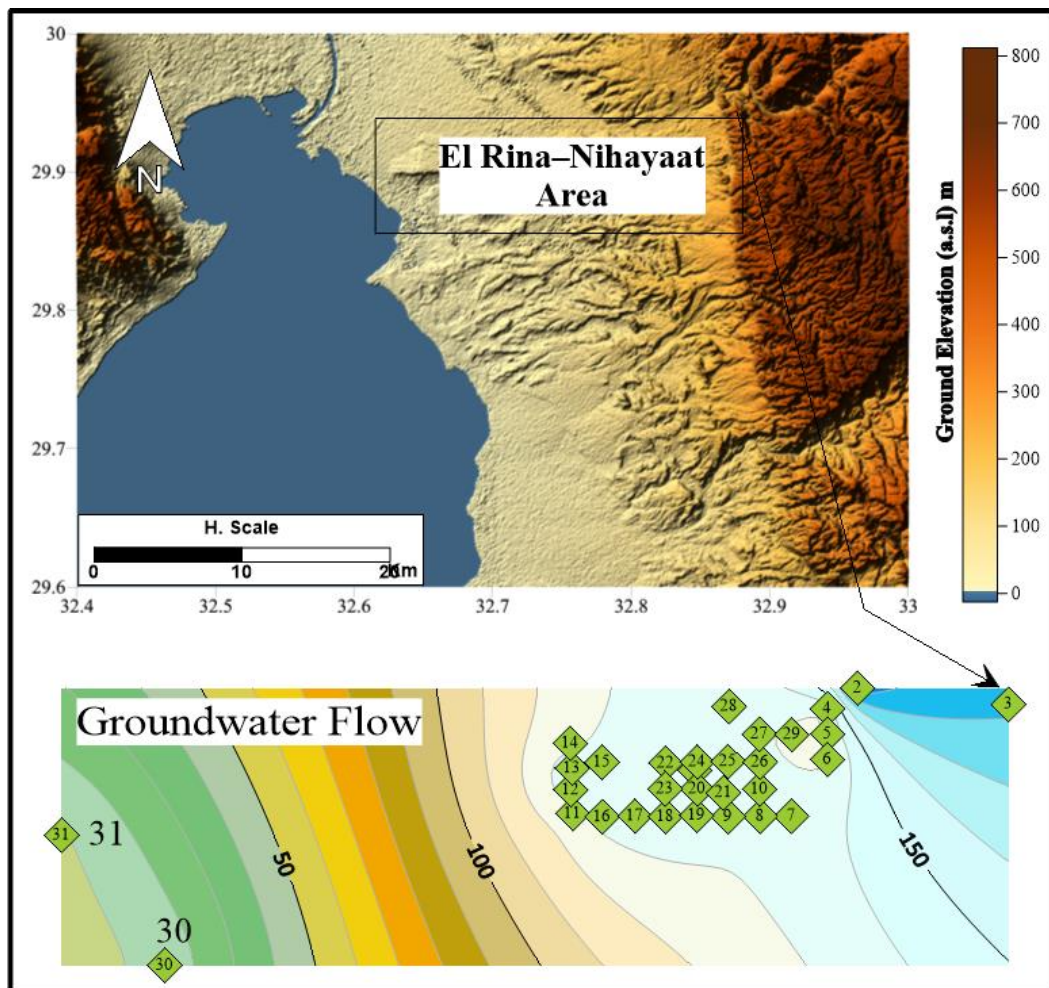


Fig. 3. Groundwater flow map of the Upper Cretaceous Aquifer, El Rina–Nihayaat, South Sinai

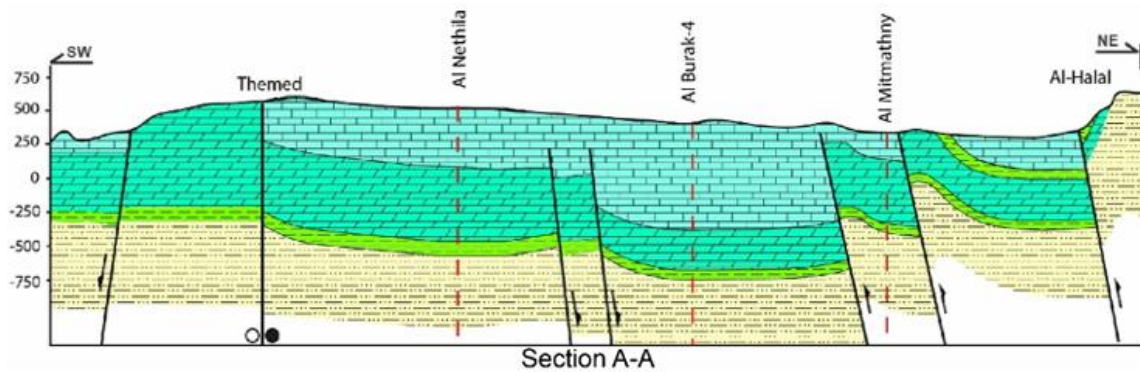


Fig. 4. Hydrogeological cross-section showing the upper cretaceous and Lower Cretaceous Aquifers (LCA) in the Sinai Peninsula [10]

This indicates that the primary source of the groundwater recharge for the fractured limestone aquifer is mainly from the eastern side of the upstream watershed of the El-Tih Plateau at Al-Halal area in the Northeastern side of the study area (Fig. 4). The aquifer is discharged mainly through the natural springs appearing close to the coast. In the central and northern Sinai, the groundwater in the LCA occurs under the confining system and the groundwater flows toward the Northwest.

3. RESULTS AND DISCUSSION

3.1 Groundwater Geochemistry

3.1.1 Geospatial distribution of groundwater salinity and major ions

The distribution of groundwater salinity and the dissolved major ions give great insights into the recharge and salinization sources as well as the impact of the aquifer matrix on the groundwater quality. The groundwater salinity ranges from 1078 (No. 8) to 13090 mg/L (No. 14), with an average value of 1839 mg/L. In Fig. 5, the contour map shows the groundwater salinity increases from the upstream close to the shed mountains toward the downstream portion of the El Rina–Nihayaat basins. Concerning the major cations, the concentration of calcium ranges between 2.4 mg/L (No.2) and 2520 mg/L (No. 14), while magnesium ranges from 11.6 mg/L (No. 22) to 1530.9 mg/L (No. 14). The main sources of calcium and magnesium are due to dissolution of marine dolomitic limestone that has been recorded in subsurface strata of the limestone aquifer including Sudr and Matullah Formations. In consequence, The dissolved sodium ions range between 93 mg/L (No. 1) and 985 mg/L (No. 31) with an average value of 322

mg/L, while potassium ranges from 18.6 mg/L (No. 5) to 120.2 mg/L (No. 21) with an average value of 42 mg/L. In Fig. 5, the contour map of Ca + Mg and Na + K, well coincides with the distribution of groundwater salinity and groundwater flow direction, which confirms the recharge source comes from the upstream watershed. Concerning the dissolved major anions; carbonate has not been detected in all groundwater samples except well No. 11 where it was 20.5 mg/L. The dissolved bicarbonate ranges from 27.8 mg/L (No.11) to 232.9 mg/L (No.31) with an average value of 68 mg/L where it increases upstream. The sulfate ions indicate the impact of leaching and dissolution from the aquifer matrix, it ranges between 8.7 mg/L (No. 16) and 398.1 mg/L (No. 4) with an average value of 79 mg/L. Chloride is considered a conservative ion, which provides great insights for mixing with different water. It ranges between 614.04 (No. 8) and 8772 mg/L (No.14) with an average value of 1075 mg/L. In Fig. 5, the spatial distribution of bicarbonate ion is inversed with the distribution of groundwater salinity and the major cations, where it decreases upstream and increases downstream, while sulfate and chloride well coincided with the salinity contour map. The main source of major ions in groundwater comes from the leaching and dissolution of clay sheets enclosed with the limestone beds as well as the leaching of marine origin deposits like limestone and chalk.

3.1.2 Origin of groundwater recharge and salinization

The Gibbs diagram has been used to investigate the origin of groundwater recharge and salinization as well as geochemical processes governing groundwater quality [45]. In Figs. 6a, and 6b the groundwater from the rainwater, UCA,

and the Lower Cretaceous aquifer have been plotted to investigate the origin of the groundwater of the UCA. The groundwater salinity plotted versus the $Cl/(Cl+HCO_3)$ and $Na/(Na+Ca)$, all groundwater wells tapping the UCA are plotted out of the precipitation, rock, and evaporation dominances, except sample Nos. 1, 14, 30, and 31. This indicates that the groundwater of the UCA has been made by a mixing between two different groundwater of diverse origins. In Fig. 6b., the groundwater tapping the Lower Cretaceous aquifer has been plotted in the zone of evaporation and close to the rock dominance. In the Piper diagram [46], all groundwater samples have been plotted in Area 7, where the Cl-Na is the main water type. Groundwater tapping the LCA, and sample No. 30 are plotted in Area 9, indicating mixed water types. However, groundwater samples No. 1, 14, and 31 from the UCA and Sudr El-Heitan sample from the LCA, have been plotted in area 6, indicating Cl-Ca water type and the impact of marine deposits. The relationships between the Cl versus salinity and other major cations give a great indication of the groundwater origin [45].

Consequently, the Cl concentration has been plotted versus the salinity, Ca, Mg, and Na to reveal the main geochemical processes controlling the groundwater quality. The groundwater samples representing the LCA, and rainwater have been used as two important end groundwater members. In Figs. 7 a, b, c, and d, the UCA groundwater has high chloride however, higher salinity, lower calcium, and magnesium concentrations relative to the LCA and rainwater end members. Most of the groundwater wells tapping the LCA have been plotted in between three end members rainwater, LCA, and sample No. 15. Rainwater represents the chemistry of the recent recharge from annual precipitation, the LCA sample represents the upward leakages from the underneath Nubian paleowater (LCA), and Sample No. 15 represents the final stage of groundwater evolution due to the water-rock interaction. Most of the groundwater tapping the UCA is plotted in between these three-end members indicating the impact and contribution of recent recharge, upward leakage, and rock-water interaction.

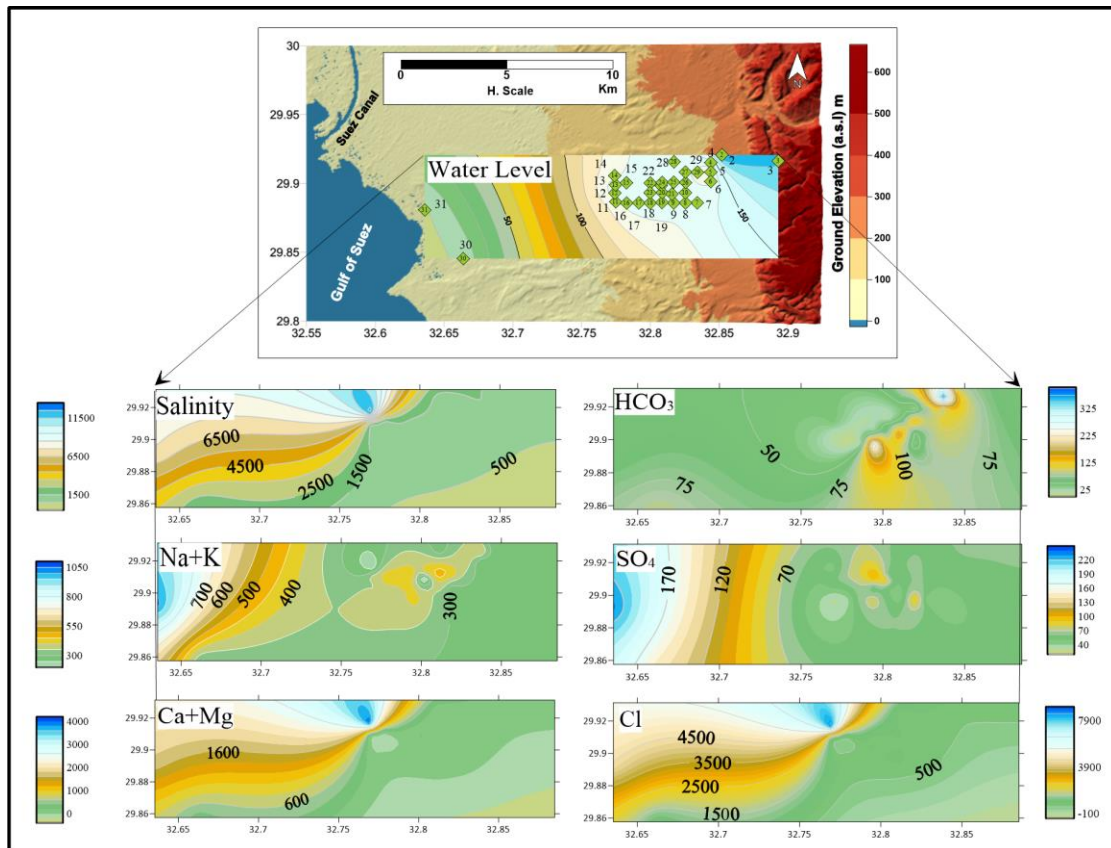


Fig. 5. Spatial distribution of salinity, major cations (Na + K, and Ca + Mg in mg/L), and major anions (HCO₃, SO₄, and Cl in mg/L) in the groundwater of the Upper Cretaceous Aquifer, El Rina-Nihayaat, South Sinai, Egypt

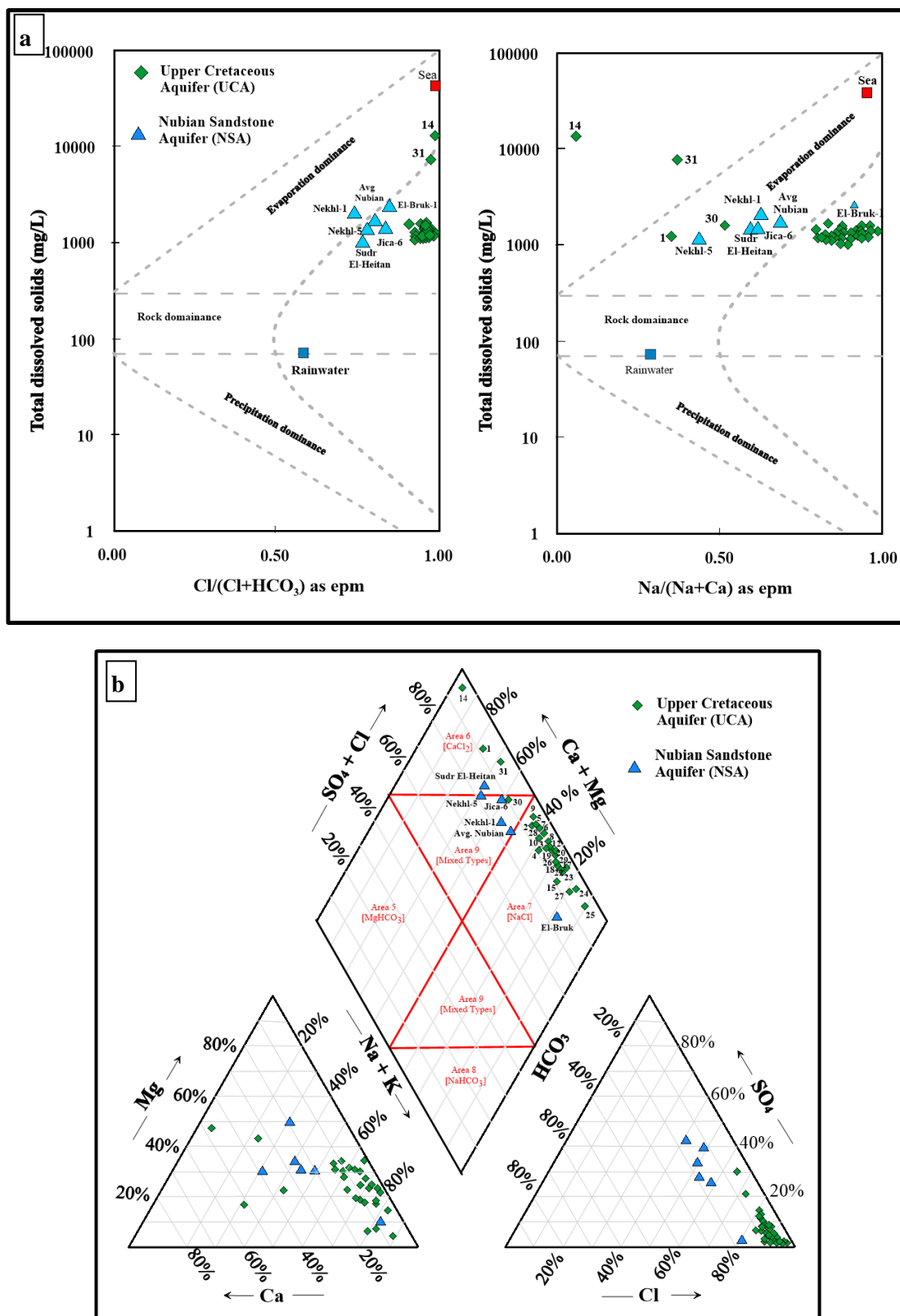


Fig. 6. a) Gibbs diagram [45], and b) Piper Diagram [46], for groundwater samples tapping the Lower and Upper Cretaceous aquifer (UCA) in the Sinai Peninsula

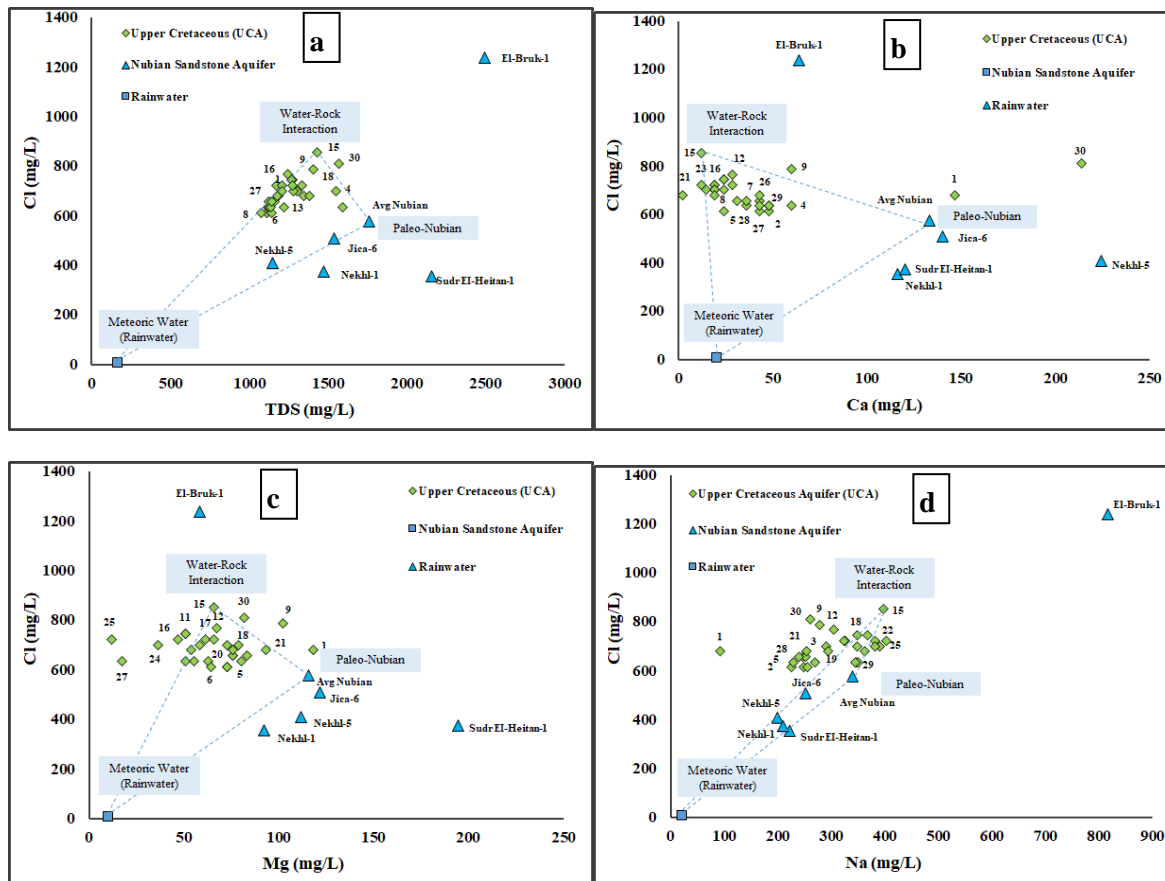


Fig. 7. Ion relationships between chloride and a) Salinity (TDS), b) Calcium c) Magnesium, and d) Sodium

3.2 Stable Isotopes for Groundwater Origin

The stable isotopes $\delta^{18}\text{O}$ and $\delta^2\text{H}$ have been measured in the groundwater samples to determine the main source(s) of recharge and salinization origin [47]. The $\delta^{18}\text{O}$ ranges between -6.37 (No. 14) and -4.43 (No. 30), while the $\delta^2\text{H}$ ranges from -40.2 (No. 30) to -28.3 (No. 31). All groundwater samples are relatively depleted with the isotopic content to the isotopic signature relative to the weighted mean average of the recent rainwater (-4.37 and -21.4) [25,12] and relatively enriched than the Nubian sandstone paleo-groundwater. In Fig. 8, the groundwater samples of the El Rina–Nihayaat area have been plotted between two end members; the recent rainwater and the paleo Nubian groundwater, where samples are directly plotted along with the Global Meteoric Water Line (GMWL) that has been described by Craig [48] (Fig. 8a).

The UCA groundwater samples show no significant enrichments due to evaporation

processes. In Figure 8b, the $\delta^{18}\text{O}$ versus the groundwater salinity, most groundwater samples are plotted in between three end members: the recent rainwater, the paleo Nubian groundwater (LCA), and sample No. 15. Sample No.15 represents the final stage of groundwater evolution, where it has high groundwater salinity and chloride concentration and highly enriched with the isotopic signature of the $\delta^{18}\text{O}$. This indicates that the primary source of groundwater recharge of the limestone aquifer is mixed sources between the underneath Nubian paleo-groundwater (LCA) and the recent precipitations.

3.3 Geochemical NETPATH Model

The geochemical NETPATH model has been used to investigate the impact of geochemical processes on the groundwater and estimate the mass transferred due to water-rock interaction and mixing with different water [28,29,49]. In this study, the NETPATH model has been run using two end members, rainwater, and paleo-Nubian water to interpret the geochemical component of

a final groundwater sample tapping the limestone aquifer at El Rina–Nihayaat area. The geochemical analyses have been used as a constraint, while the rock forming the aquifer matrix of the limestone aquifer has been used as input phases (Table 2). Carbonate minerals including calcite and dolomite are used as phases as the aquifer strata are composed mainly of limestone and dolomitic in Sudr and Matullah Formations of marine origin. The sulfate mineral (gypsum) and halite have been included in the model to represent the evaporites intercalated with shale in the Ras Malaab Formation (Vadose aquifer zone). Clay minerals (illite, montmorillonite, kaolinite, and chlorite) were used as the UCA aquifer is mainly intercalated with clay and shale of Esna shale of Eocene age. The saturation indices for different minerals have been estimated using the WATEQ to determine the dissolved and precipitated minerals within the groundwater flow path (Table 3). The model has been calibrated using the saturation indices values for different minerals to be sure the estimated mass transferred coincided with the preceding geochemical reaction. Based on the cross-section in Fig. 4, the Nubian Sandstone aquifer underneath the fractured limestone aquifer and the stable isotopes show mining and upward leakages from the paleo-Nubian groundwater. Therefore, the historical geochemical data have been collected from the nearby wells representing the Nubian paleo groundwater and used as input data for the NETPATH geochemical model. The models show precipitations of calcite, clay minerals (montmorillonite and chlorite), and dissolution of gypsum, dolomite, halite, and silica with reverse cation exchange (Table 4). The estimated mixing percentages from the Nubian Sandstone aquifer range between 11.5% to 49.8% while the mixing percentages from the rainwater end member range between 18.1 % to 88.5%. The main sources of groundwater recharge are the upward leakages from the Nubian aquifer and the annual precipitation that comes from the El-Tih plateau located in the central Sinai watershed where the UCA crops out at the surface. The mixing ratios between the rainwater and the paleo Nubian groundwater have been estimated using the $\delta^{18}\text{O}$ data in the mixing equation described by Faure [50]; Clark [51]. The average $\delta^{18}\text{O}$ in the Nubian groundwater samples (Nekhel-1, Nekhel-5, Jica-6, Sudr Heitan-1, and El-Bruk-1) and the weighted mean average of the recent precipitation estimated by Eissa et al. [12] were used to estimate the upward leakages from paleo-Nubian and the mixing percentages from

the recent rainwater, respectively. Fig. 9 shows most of the estimated mixing percentages from $\delta^{18}\text{O}$ which are very close to the estimated percentage by the NETPATH. In the schematic hydrogeological cross-section (Fig. 10), the aquifer is confined by thick clay sheets that have been locally recorded in the study area. Therefore, the meteoric recharge for the aquifer mainly comes from remote watersheds (ie. El-Tih Plateau) where the Eocene rocks crop out and recharged from the upward leakages of the underneath Nubian Sandstone Aquifer (NSA) through the deep-seated faults.

3.4 Factorial Analysis

Statistical analyses have been used to correlate the hydrogeochemical composition of groundwater which is known to have mutual relationships. The factorial analyses and proven highly efficient in groundwater chemistry to find smaller factors that describe the geochemical processes that influence the groundwater quality [52-54]. The techniques investigate the geospatial relationship between variables (salinity and major ions) and describe different sampling sites. The KeyPlot program developed by Yoshioka [30] has been used to estimate the main factors using the major ions (Ca^{2+} , Mg^{2+} , Na^+ , K^+ , SO_4^{2-} , HCO_3^- and Cl^-) and groundwater salinity as an input data set. The multivariate groundwater datasets were reduced to three main factors which explain 87.8% of the total variances of the input data using Varimax data rotation (Fig. 11). Factor 1 describes 31.9% of the total variance whereas it has strong positive loading for Mg (0.82), Ca (0.68), and HCO_3^- (0.4). Factor 2 represents 30 % of the data set. It has strong positive loading for SO_4 (0.95), TDS (0.81), and K (0.59). Factor 3 represents 25.8 % of the data set. It has strong positive loading for Cl (0.95), salinity (0.58), and Na (0.36). Factor 1 indicates the impact of meteoric recharge where it has been linked with the HCO_3^- ions as well as the leaching of carbonate minerals including dolomite and calcite that are embedded in the aquifer matrix and dominating the Upper cretaceous rock (i.e. Sudr and Matullah). Additionally, the spatial distribution of Factor 1, increases with the groundwater flow direction indicating recharge origin. Factor 2 shows the impact of water-rock interaction due to the leaching of terrestrial deposits while Factor 3 is mainly due to the upward leakage from the underneath Nubian paleowater.

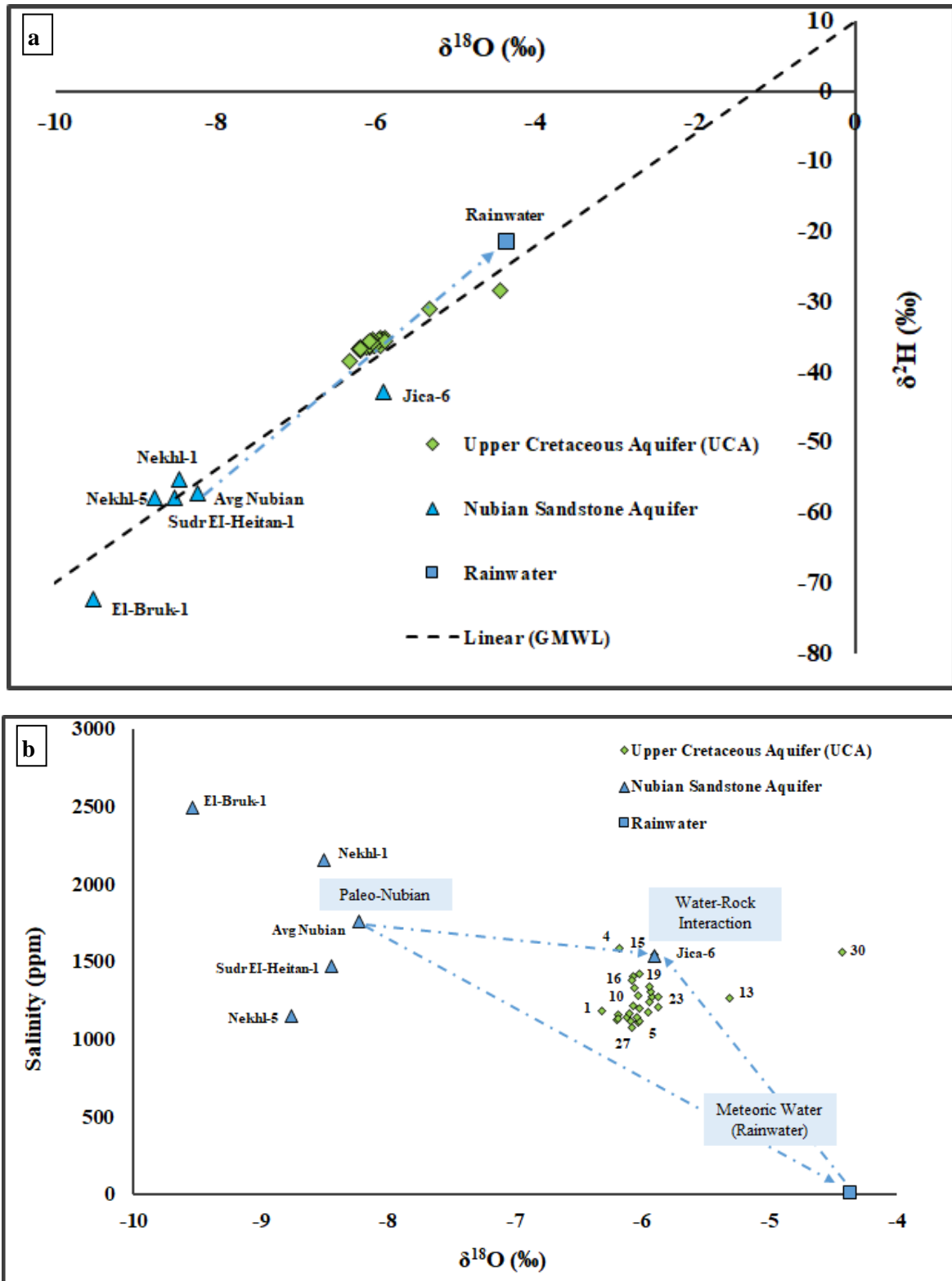


Fig. 8. Relationships between $\delta^{18}\text{O}$ (‰) versus; a) Deuterium ($\delta^2\text{H}$) (‰) and b) Salinity (mg/L) for groundwater samples tapping the Lower and Upper Cretaceous aquifer (UCA) in the study area

Table 2. Mineral saturation indices for phases in NETPATH geochemical models

Aquifer	Well No.	Cal	Dol	Gyp	SiO ₂	Hal	Illt	Mont	Kaol	Chlrt
Nubian Sandstone Aquifer (NSA)	1	0.466	1.243	-1.782	-1.107	-3.91	1.168	0.912	2.564	4.166
	4	-0.276	-0.256	-1.343	-1.021	-3.37	2.507	2.112	3.608	1.619
	6	-0.041	0.514	-1.955	-1.135	-3.53	0.460	0.013	1.823	4.934
	11	-0.723	-0.722	-3.022	-1.103	-3.28	1.084	0.693	2.455	3.199
	12	-0.090	0.585	-2.927	-1.109	-3.35	0.716	0.083	1.843	6.148
	15	-0.602	-0.038	-3.098	-1.128	-3.18	0.642	0.189	2.076	4.147
	16	-0.961	-1.110	-3.374	-1.124	-3.34	0.993	0.858	2.699	1.144
	17	-0.308	0.314	-3.020	-1.129	-3.34	0.527	0.053	1.903	4.843
	18	-0.749	-0.600	-1.983	-1.024	-3.31	2.810	2.363	3.945	0.717
	21	-1.071	-0.153	-3.076	-1.125	-3.48	0.667	-0.673	1.307	8.377
	30	0.251	0.458	-1.510	-1.078	-3.39	2.104	2.327	3.888	-1.230
	Avg.	-0.071	0.164	-1.158	-1.077	-3.43	2.214	2.846	4.452	-3.159
Nubian Rainwater		-1.684	-3.302	-2.503	-1.781	-5.2	-0.598	0.275	3.138	-9.318

Note: Cal. Calcite; Dol. Dolomite; Gyp. Gypsum; SiO₂. Silica; Hal. Halite; Illt. Illite; Mont. Montmorillonite; Kaol. Kaolinite; Chlrt. Chlorite; C/Ex. Cation Exchange; -- Not included

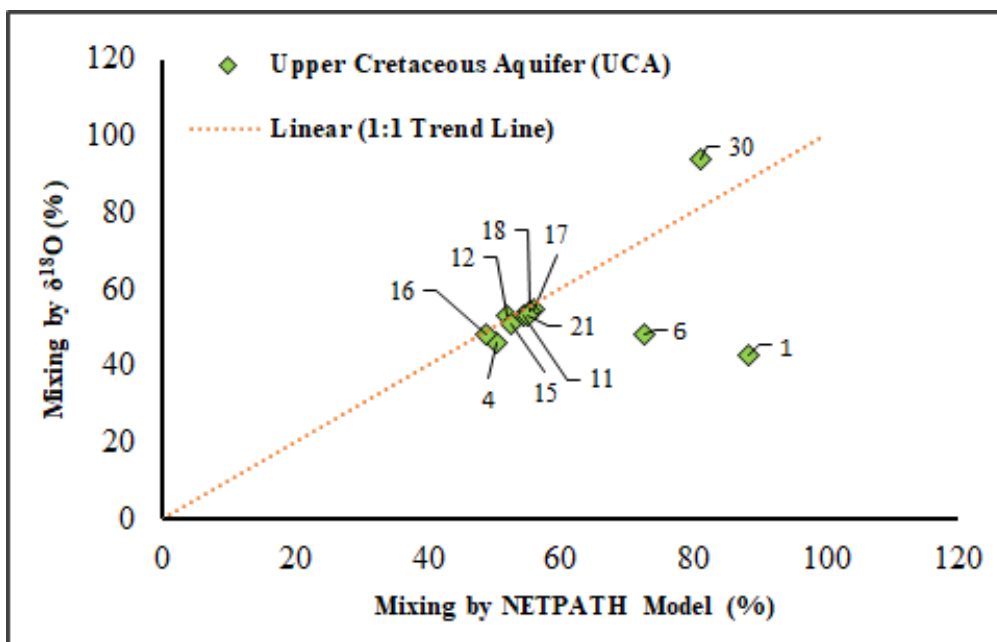


Fig. 9. Relationship between the estimated mixing percentage using the NETPATH model and the $\delta^{18}\text{O}$ (‰)

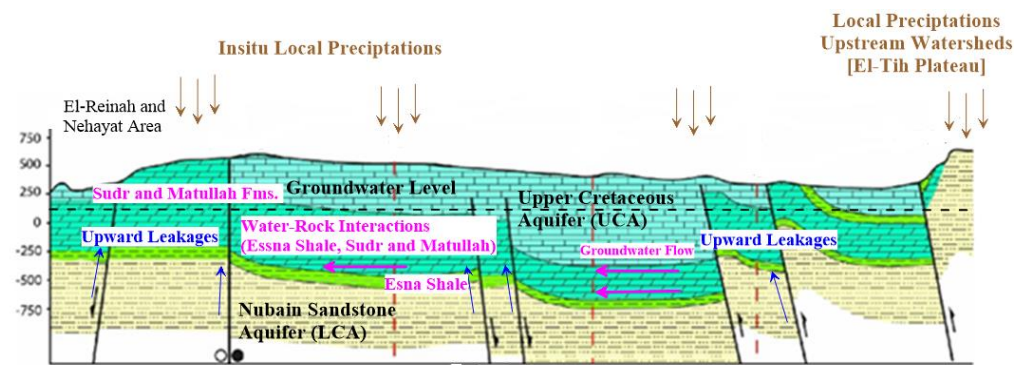


Fig. 10. Schematic diagram showing the recharge mechanism and the water-rock interaction of the upper Cretaceous Aquifer

Table 3. Constraints, phases, and physical parameters used as input data in the NETPATH geochemical model

Constrains	Phases	Parameters
Calcium, Carbon, Chloride, Magnesium, Potassium, Sodium, Sulfur, Silica.	Calcite, Dolomite, Gypsum, Silica, Halite, Illite, Montmorillonite, Kaolinite, Chlorite and Exchange,	Mixing (Yes) Evaporation (No) Exchange (Yes)

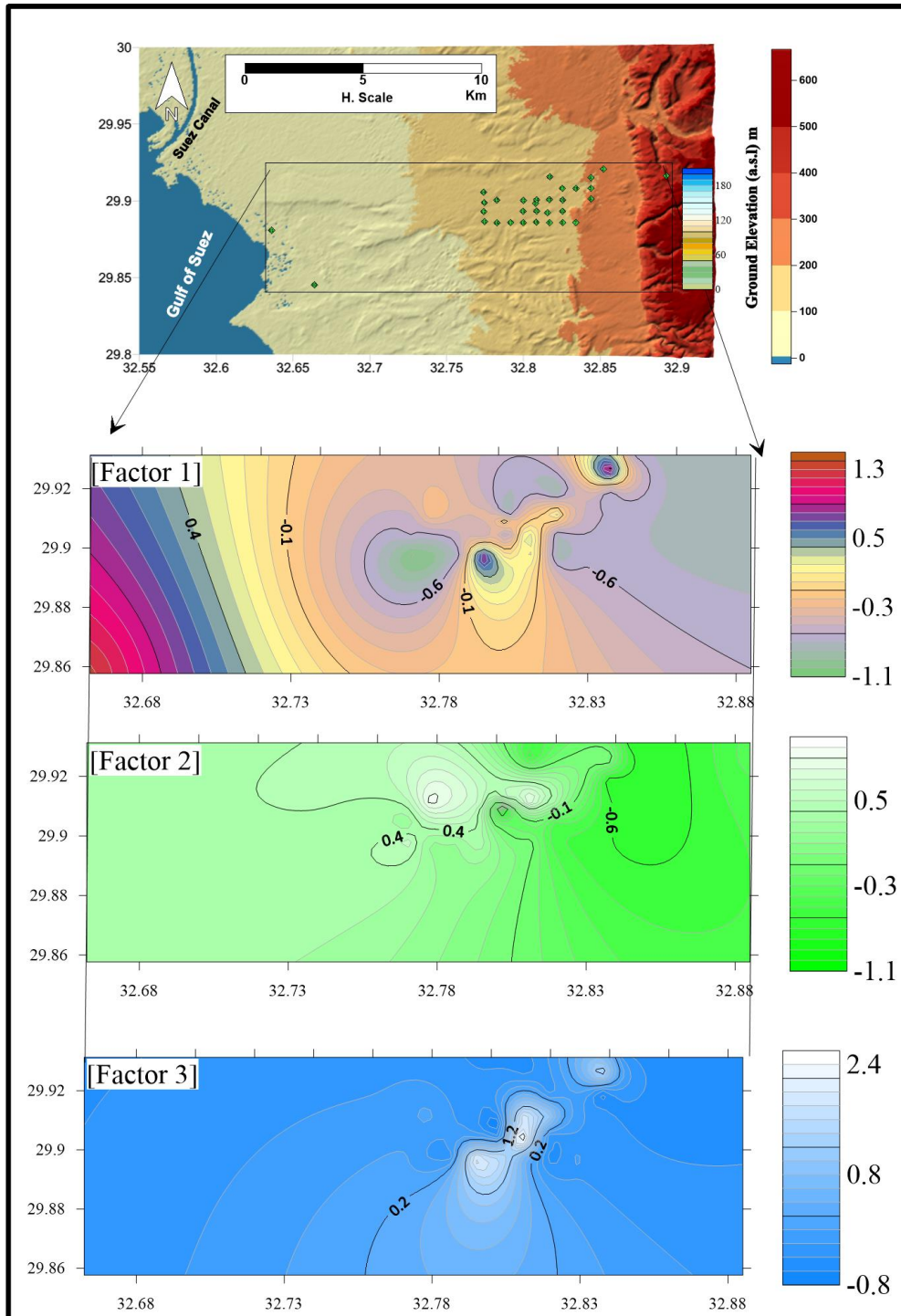


Fig. 11. Spatial distribution of the factorial analyses for groundwater samples in the study area

Table 4. NETPATH modeling results (mmol/L) for the El Rina–Nihayaat Positive values mean the phase is going into solution, while negative values mean the phase is being removed from the solution

Initial Water #1	Initial Water # 2	Estimated Mixing (%) by NETPATH		Final Water	Cal	Dol	Gyp	SiO ₂	Hal	Ill	Mont	Kaol	Chlrt	C/Ex	Estimated Mixing (%) by δ ¹⁸ O	
		Rainwater	Paleo-Nubian												Rainwater	Paleo-Nubian
Rainwater	Average of Paleo-Nubian Groundwater	88.5	11.5	1	-9.6	5.24	--	5.18	17.08	0.67	-4.26	2.31	--	--	43	57
		50.2	49.8	4	-2.01	--	2.2	14.61	9.69	--	-10.85	10.59	--	-1.22	46	54
		72.6	27.4	6	-5.91	2.55	--	0.82	12.67	1.26	-1.18	--	-0.27	-3.28	48	52
		54.5	45.5	11	-1.41	-0.57	-1.63	0.21	13.4	1.12	-1.19	--	--	-2.35	53	47
		51.9	48.1	12	-1.9	--	-1.7	10.63	13.69	1.03	-8.8	9.07	--	-3.99	53	47
		52.5	47.5	15	-8.49	4.7	--	0.18	23.85	1.1	-0.62	--	-0.53	-3.69	51	49
		48.6	51.4	16	-2.43	--	-1.91	3.58	11.91	2.91	-0.01	--	--	-2.87	48	52
		56	44	17	-1.44	--	-1.52	9.46	--	0.82	-7.74	-3.0	--	--	55	45
		55.3	44.7	18	-1.51	--	1.03	22.51	12.37	3.53	-19.91	19.13	--	-2.16	54	46
		55.1	44.9	21	-2.54	0.29	--	21.41	11.72	4.72	-20.16	18.05	--	-3.91	53	47
		81.1	18.9	30	-4.53	3.11	--	0.22	19.6	1.2	-1.02	--	-0.25	-5.89	94	6

Note: Cal. Calcite; Dol. Dolomite; Gyp. Gypsum; SiO₂. Silica; Hal. Halite; Ill. Illite; Mont. Montmorillonite; Kaol. Kaolinite; Chrt. Chlorite; C/Ex. Cation Exchange; -- Not included

4. CONCLUSION

El Rina–Nihayaat is located within the arid region in South Sinai, Egypt. Groundwater in the Upper Cretaceous aquifer (UCA) is the main source of water for irrigation and developmental projects. Groundwater geochemistry investigates the spatial distribution of chemical constituents dissolved in water, including major ions (calcium, magnesium, sodium, potassium, chloride, sulfate, bicarbonate). The groundwater in the UCA is mainly brackish water type. The groundwater flows toward the Gulf of Suez, and the groundwater salinity, major cations, sulfate, and chloride increase from the upstream watersheds toward the downstream. Based on the Gibbs and Piper diagrams, the groundwater evolved due to water-rock interaction and mixing with different water origins. The ion ratios (Cl versus salinity, Ca, Mg, and Na) in most of the groundwater samples have been altered due to water-rock interaction and mixing with meteoric water (rainwater) and the paleo-Nubian upward leakage. Geochemical and isotopic techniques aid in identifying the sources and rates of groundwater recharge, as well as understanding how water moves through aquifers. The stable isotopes ($\delta^{18}\text{O}$ and $\delta^2\text{H}$) content in the UCA is relatively depleted relative to the weighted mean average of the recent rainwater and enriched relative to the average paleo-Nubian groundwater in the underneath Lower Cretaceous aquifer, confirming the mixing of both end members. The NETPATH geochemical model estimates the mass transferred within the groundwater flow path from upstream toward downstream and confirms the mixing between meteoric and paleowater origin. The estimated mixing percentages from the rainwater range between 48.6 % and 88.5 %, while the upward leakages from the underneath Nubian groundwater range between 11.5 % to 51.4 %. The factorial analyses indicate three main factors governing the geochemistry of groundwater in the UCA: including water-rock interactions, meteoric recharge from annual precipitation, and upward leakages from the underneath paleowater.

ACKNOWLEDGEMENT

Authors acknowledge the Science and Technology Development Fund (STDF) FLUG Call 1 - Project ID 46655, for supporting this work including the fieldwork that has been carried out and chemical analyses of water samples.

COMPETING INTERESTS

Author has declared that no competing interests exist.

REFERENCES

1. Dames M. Sinai development study–phase I, final report, Water Supplies and Costs. Volume V-Report Submitted to the Advisory Committee for Reconstruction, Ministry of Development. Cairo; 1985.
2. IGRAC. Transboundary aquifers of the world, Update 2021, Scale 1:50 000 000, Special edition for the 5th World Water Forum, Istanbul; 2009.
3. Nour S. Hydrogeology of deep aquifers in the Western Desert and Sinai, Report No.10, Water policy reform activity, U S Agency for International Development, Ministry of Public Works and Water Resources, Egypt; 1998.
4. El-Bihery MA. Water resources and sustainable development in Sinai Peninsula-Egypt, Ph.D. thesis, Geology Department, Faculty of Science, Ain Shams University, Egypt; 1998.
5. Botros FEF. Groundwater modeling for deep lower cretaceous aquifer system in Sinai, M.Sc. Thesis, Faculty of Engineering, Cairo University, Egypt; 2003.
6. El Rahman HA. Evaluation of groundwater resources in Lower Cretaceous aquifer system in Sinai. *Water Resources Management*. 2001;15(3):187–202
7. Ghoubachy SY. Contribution to the hydrogeology of the Lower Cretaceous aquifer in east Central Sinai, Egypt. *Journal of King Saud University- Science*. 2013;25(2):91-105.
8. JICA. North Sinai groundwater resources study in the Arab Republic of Egypt, Japan International Cooperation Agency, Final Report; 1992.
9. JICA. South Sinai groundwater resources study in the Arab Republic of Egypt, Japan International Cooperation Agency, Final Report; 1999.
10. Ibrahim HA, Abd-Elmegeed MA, Ghanem AM, Hassan AE. Assessment of groundwater development potential in Upper Cretaceous aquifer in Sinai, Egypt. *Arabian Journal of Geosciences*. 2021;14: 1-3.
11. Rosenthal E, Zilberbrand M, Livshitz Y. The hydrochemical evolution of brackish groundwater in central and northern Sinai

- (Egypt) and in the western Negev (Israel). *Journal of Hydrology*. 2007;337(3-4):294-314.
12. Eissa MA, Thomas JM, Hershey RL, Dawoud MI, Pohl G, Gomaa MA, Kamal AD, Geochemical and isotopic evolution of groundwater in the Wadi Watir Watershed, Sinai Peninsula, Egypt. *Environ Earth Science*. 2013;71:1855-1869
 13. Kotb A, Mosaad S, Kehew AE. Geophysical and hydrogeological applications for groundwater evaluation, east El-Minia area, upper Egypt. *Journal of African Earth Sciences*. 2021;184:104384
 14. Flores YG, Eid MH, Szűcs P, Szócs T, Fancsik T, Szanyi J, Kovács B, Markos G, Újlaki P, Tóth P, McIntosh RW. Integration of geological, geochemical modelling and hydrodynamic condition for understanding the geometry and flow pattern of the aquifer system, Southern Nyírség-Hajdúság, Hungary. *Water*. 2023;15(16):2888
 15. Ahmed M, Chen Y, Khalil MM. Isotopic composition of groundwater resources in arid environments. *Journal of Hydrology*. 2022;609:127773.
 16. Samy A, Eissa M, Shahen S, Said MM, Abou-Shahaba RM. Solute transport and geochemical modeling of the coastal quaternary aquifer, Delta Dahab Basin, South Sinai, Egypt. *Acta Geochimica*. 2023;29:1-24
 17. Wannous M, Theilen-Willige B, Troeger U, Falk M, Siebert C, Bauer F. Hydrochemistry and environmental isotopes of spring water and their relation to structure and lithology identified with remote sensing methods in Wadi Araba, Egypt. *Hydrogeology Journal*. 2021;29(6):2245-2266
 18. Greenwood NH The Sinai: A physical geography. University of Texas Press, Austin, TX; 1997.
 19. Eissa MA, Thomas JM, Pohl G, Shouakar-Stash O, Hershey RL, Dawoud M. Groundwater recharge and salinization in the arid coastal plain aquifer of the Wadi Watir delta, Sinai, Egypt. *Applied Geochemistry*. 2016;71:48-62
 20. Omar AE, Abdel-Halim KA, Arnous MO. State of the Practice Worldwide: Utilizing hydrogeochemical data and GIS tools to assess the groundwater quality in arid region: Example from Wadi Feiran basin, Southwestern Sinai, Egypt. *Groundwater Monitoring & Remediation*; 2023. Available: <https://doi.org/10.1111/gwmr.12625>
 21. Dassi L, Tarki, M, El Mejri H, Ben Hammadi M. Effect of overpumping and irrigation stress on hydrochemistry and hydrodynamics of a Saharan oasis groundwater system. *Hydrological Sciences Journal*. 2018;63(2):227-250
 22. Mohamed L. Structural controls on the distribution of groundwater in southern Sinai, Egypt: constraints from geophysical and remote sensing observations. *Dissertations Paper 593*; 2015. DOI: <http://scholarworks.wmich.edu/dissertations/593>
 23. GeoEngineers. Inc. Soil and groundwater assessment, Ellensburg, Washington. August 2nd, 2021. GEI File Number 0504-169-00; 2021.
 24. Fishman MJ, Friedman LC. Methods for the determination of inorganic substances in water and fluvial sediments. *USGS Tech Water Resour Invest. book 5, chapter A1*, USGS, Reston, VA; 1989.
 25. Hem JD. Study and interpretation of the chemical characteristics of natural water. 3rd ed. Scientific Publication Jodhpur, India. 1991;2254.
 26. IAEA, Stable isotope hydrology: Deuterium and oxygen-18 in water cycle. In: Gat JR, Gonfiantini R (eds), Technical report no. 210, International Atomic Energy Agency, Vienna. 1981;339.
 27. Morrison J, Brockwell T, Merren T, Fourel F, Phillips AM, On-line high-precision stable hydrogen isotopic analyses on nanoliter water samples. *Anal Chem*. 2001; 73:3570-3575
 28. Plummer LN. Geochemical modeling of water-rock interaction: Past, present, future. In: Kharaka YK, Maest AS (eds) *Water-rock interaction*. Balkema, Rotterdam. 1992;23-33.
 29. Plummer LN, Prestemon EC, Parkhurst DL. An interactive code (NETPATH) for modeling net geochemical reactions along a flow path, version 2.0. *US Geol Surv Water Resour Invest Rep*. 1994;94-4169:130.
 30. Yoshioka K. Ky Plot Program Version 2.0. www.phy.gonza.ga.Edu; 2001.
 31. Shalaby Y, Embaby A, Siam A. Structural constraints on the groundwater regime of the Cretaceous aquifers in Central Sinai, Egypt. *Journal of African Earth Sciences*. 2012;75:37-56

32. Jenkins DA. North and central Sinai. In: Said R (ed) The geology of Egypt. Balkema, Rotterdam/Brookfield. 1990;361-380.
33. Bartov Y, Lewy Z, Steinitz G, Zak I. Mesozoic and tertiary stratigraphy, paleogeography and structural history of Gebel Arif El Naga area, Eastern Sinai. Israel Journal of Earth Sciences. 1980; 29(1-2):114-139
34. El-Ghazawi MM Hydrogeological studies in northeast Sinai, Egypt. Ph.D. Thesis, El-Mansoura Univ., Egypt. 1989;290.
35. Agah A. Structural map and plate reconstruction of the Gulf of Suez- Sinai area. Internal Report, Conoco Oil Co., Houston, Texas, U.S.A; 1981.
36. Hassanein AM, Geological and Geomorphological impacts on the water resources in central Sinai, Egypt. Ph.D. Thesis, Ain Shams Univ., Egypt. 1997;373.
37. CONOCO Continental Oil Company Geologic map of Egypt (Scale 1:500,000). CONOCO, Houston, TX; 1987.
38. Shata A. Geomorphological aspects of the western Sinai foreshore. Bull. de l'Institute due Desert. 1955;5.
39. Massoud U. Geophysical studies for groundwater exploration in El-Bruk area, north central Sinai, Egypt. PhD Thesis, Minoufiya Univ., Egypt. 2005;130.
40. JICA. North Sinai groundwater resources study in the Arab Republic of Egypt, Japan International Cooperation Agency, Final Report; 1992.
41. JICA. South Sinai groundwater resources study in the Arab Republic of Egypt, Japan International Cooperation Agency, Final Report; 1999.
42. EGSMA (Egyptian Geological Survey and Mining Authority). Geological map of El-Hassana quadrangle, Sinai, Egypt. Scale 1: 100,000, EGSMA, Cairo; 1993.
43. Aggour TA, Hewidy, AA, Attia SH, Abu El F ettouh MA, Yousif M, Geology of water resources at Wadi Geraia basin, Sinai, Egypt. Egyptian Journal of Geology. 2007;51:177-204.
44. Massoud U, Santos F, Khalil MA, Taha A, Abbas AM. Estimation of aquifer hydraulic parameters from surface geophysical measurements: a case study of the Upper Cretaceous aquifer, central Sinai, Egypt. Hydrogeology Journal. 2010;18:699-710.
45. Gibbs RJ, Mechanisms controlling world water chemistry. Science. 1970;170:795-840
46. Piper A. A graphic procedure in the geochemical interpretation of water analyses. Transactions, American Geophysical Union. 1944;25 (6):914-928
47. Clark I, Fritz P. Environmental isotopes in hydrogeology. Lewis, New York; 1997.
48. Craig H. Isotopic variations in meteoric waters. Science. 1961;133:1702-1703
49. Hershey RL, Heilweil VM, Gardner P, Lyles B, Earman S, Thomas J, Lundmark KW, Ground-water chemistry interpretations supporting the Basin and Range Regional Carbonate-rock Aquifer System (BARCAS) Study, eastern Nevada and western Utah. DHS Publication No. 41230. Prepared by Desert Research Institute, Nevada System of Higher Education, Reno, NV, and US Geological Survey, Reston, VA; 2007.
50. Faure G. Principles of Isotope Geology, second ed. Wiley, New York; 1986.
51. Clark I. Groundwater Geochemistry, and Isotopes. CRC Press, Boca Raton, Florida; 2015.
52. Liu CW, Lin KH, Kuo YM. Application of factor analysis in the assessment of groundwater quality in a Blackfoot disease area in Taiwan. Science of the total environment. 2003;313(1-3):77-89.
53. Love D, Hallbauer D, Amos A, Hranova R. Factor analysis as a tool in groundwater quality management: two southern African case studies. Physics and Chemistry of the Earth. 2004;Parts A/B/C,29(15-18):1135-1143
54. Varol S, Davraz A. Evaluation of the groundwater quality with WQI (Water Quality Index) and multivariate analysis: A case study of the Tefenni plain (Burdur/Turkey). Environmental earth sciences. 2015;73:1725-1744

© 2024 Eissa; This is an Open Access article distributed under the terms of the Creative Commons Attribution License (<http://creativecommons.org/licenses/by/4.0>), which permits unrestricted use, distribution, and reproduction in any medium, provided the original work is properly cited.

Peer-review history:

The peer review history for this paper can be accessed here:

<https://www.sdiarticle5.com/review-history/112097>